Int. J. Heat Mass Transfer. Vol. 31, No. 5, pp. 957–967, 1988
Printed in Great Britain

0017–9310/88 $3.00 + 0.00
Pergamon Press plc

Detailed study of a model of heat and mass transfer during convective drying of porous media

S. BEN NASRALLAH and P. PERRE

Laboratoire d'Etudes des Systèmes Thermiques et Energétiques, U.A. CNRS 1098, G.R.C. 72, 40, Avenue du Recteur Pineau, 86022 Poitiers Cédex, France

(*Received* 4 *February* 1987 *and in final form* 13 *August* 1987)

Abstract—The model of heat and mass transfer in porous media used here is deduced from Whitaker's theory. It leads to a very comprehensive set of equations and takes into account the effect of the gaseous pressure. It is numerically solved with unidirectional transfers. The evolution of temperature, moisture content and pressure as well as the overall drying kinetics are calculated for two very different porous media. This device permits to study the sensitivity of the model to internal parameters and conditions at the interface as well as the effect of certain reductions in the model.

1. INTRODUCTION

CONVECTIVE drying is usually encountered in many industrial fields (food industry, building industry, forest products, ...). Therefore, the study of this type of problem becomes very important and for several decades now has attracted the attention of several authors. Among the works relating to this question we cite the works of Whitaker [1–3] and of Bories *et al.* [4], of Moyne and Degiovanni [5] concerning drying at high temperature that of Basilico and Martin [6] and Plumb *et al.* [7] for the drying of wood, of Harmathy [8] and Huang *et al.* [9, 10].

Our contribution consists in the theoretical study of unidirectional heat and mass transfer during the drying of porous media. The model used is drawn from the work of Whitaker [1] and leads to a very comprehensive set of equations, with three variables (temperature, moisture content and pressure). We note that the effect of pressure has been considered, to our knowledge, only in cases of drying at high temperature [5] and in cases where the initial moisture content is rather weak [7–9].

This model is solved numerically for two very different porous media. This choice permits to pinpoint the effect of all the physical characteristics.

The numerical simulation enables one to determine the evolution of temperature, moisture content, and pressure as well as the overall drying kinetics.

Further, a study of the sensitivity of the model to transport parameters and conditions at the interface enables one to select those which have to be determined in detail.

We also propose certain reductions in the model:

(a) in all the simulated cases, heat transfer by convection is negligible;

(b) given certain conditions (detailed in the text) one can dispense with Darcy's law and the continuity equation of the gaseous phase.

2. FORMULATION OF THE PROBLEM

The configuration is that of a flat porous slab constituted with a solid phase that is inert and rigid, a liquid phase (pure water) and a gaseous phase which contains both air and water vapour. One side of this slab is exposed to an air flux with fixed characteristics (velocity, temperature and relative humidity). The other, adiabatic and impervious, can also represent a plane of symmetry (Fig. 1). Initially, the porous medium is isothermal and at hydrostatic equilibrium.

The theoretical formulation of heat and mass transfer in porous media is usually obtained by a change in scale. We pass from a microscopic view where the size of the representative volume is small with regard to the pores, to a macroscopic view where the size of the representative volume ω is large with regard to the pores.

The macroscopic equations are obtained by averaging the classical fluid mechanics, diffusion and transfer equations over the averaging volume ω. The average of a function f is

$$\bar{f} = \frac{1}{\omega}\int_{\omega} f \, d\omega \tag{1}$$

and the intrinsic average over a phase i is

$$\bar{f}^i = \frac{1}{\omega_i}\int_{\omega} f \, d\omega. \tag{2}$$

Given Whitaker's theory [1], the macroscopic equations governing heat and mass transfer in porous media are given in the following sections.

2.1. *Generalized Darcy's law*

Darcy's law is extended by using relative permeabilities. For the gaseous phase, since no gravitational effect is noted

NOMENCLATURE

C_p	specific heat [J kg^{-1} K^{-1}]
D_{eff}	effective diffusivity [m^2 s^{-1}]
D_r	drying rate [kg m^{-2} s^{-1}]
g	gravitational constant [m s^{-2}]
H_r	ambient relative humidity
Δh_{vap}	latent heat of evaporation [J kg^{-1}]
K	intrinsic permeability [m^2]
K_g, K_l	relative permeabilities of gas and liquid
L	thickness of the porous medium [m]
M	molar mass [kg mol^{-1}]
$\dot{m}$	evaporation rate [kg m^{-3} s^{-1}]
P	pressure [Pa]
R	universal gas constant [J mol^{-1} K^{-1}]
S	relative saturation
T	temperature [°C or K]
t	time [s]
Δt	time increment [s]
U	moisture content [kg of water/kg of solid]
v	velocity [m s^{-1}]
x	distance [m]
Δx	thickness of control volume [m]
δx	distance between two adjoining nodes [m].

Greek symbols

α	heat transfer coefficient [W m^{-2} K^{-1}]
β	mass transfer coefficient [m s^{-1}]
ε	porosity
λ_{eff}	effective thermal conductivity [W m^{-1} K^{-1}]
μ	dynamic viscosity [kg m^{-1} s^{-1}]
ν	cinematic viscosity [m^2 s^{-1}]
ρ	density [kg m^{-3}]
σ	surface tension [N m^{-1}]
ω	averaging volume [m^3].

Subscripts

a	air
atm	atmospheric
c	capillary
cr	critical
eq	equilibrium
g	gas
i	spatial index
ir	irreducible
l	liquid
psf	fibre saturation point
s	solid
sat	saturated
v	vapour
vs	saturate vapour
∞	ambient.

Superscripts

g	intrinsic average over the gaseous phase
l	intrinsic average over the liquid phase
n	time index
$\bar{}$	average value.

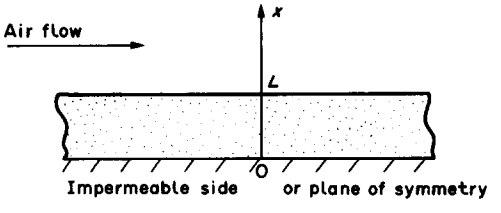

FIG. 1. Geometrical configuration.

$$\bar{v}_g = -\frac{KK_g}{\mu_g}\frac{\partial}{\partial x}(\bar{P}_g^g) \tag{3}$$

where $\bar{v}_g$ is the speed of the gaseous phase, K the intrinsic permeability, K_g the relative permeability to the gaseous phase, $\bar{P}_g^g$ the average intrinsic pressure of the gaseous mixture, and μ_g the viscosity of the gaseous phase.

For the liquid phase

$$\bar{v}_l = -\frac{KK_l}{\mu_l}\frac{\partial}{\partial x}(\bar{P}_g^g - \bar{P}_c^l + \bar{\rho}_l^l g) \tag{4}$$

where $\bar{v}_l$ is the speed of the liquid phase, K_l the relative permeability to the liquid phase, P_c the capillary pressure, μ_g the vicosity of the liquid, g the gravitational constant, and ρ_l the density of liquid.

2.2. *Mass conservation equations*

For the liquid

$$\frac{\partial \bar{\rho}_l}{\partial t} + \frac{\partial}{\partial x}(\bar{\rho}_l^l \bar{v}_l) = -\dot{m} \tag{5}$$

where $\dot{m}$ is the evaporated water in units of time and volume.

For the vapour

$$\frac{\partial \bar{\rho}_v}{\partial t} + \frac{\partial}{\partial x}(\bar{\rho}_v^g \bar{v}_v) = \dot{m} \tag{6}$$

where

$$\bar{\rho}_v^g \bar{v}_v = \bar{\rho}_v^g \bar{v}_g - \bar{\rho}_g^g D_{eff}\frac{\partial}{\partial x}(\bar{\rho}_v/\bar{\rho}_g) \tag{7}$$

$\bar{\rho}_v$ and $\bar{\rho}_g$ are the average densities of the water vapour and of the gaseous mixture, D_{eff} the coefficient of the effective diffusion of vapour in the porous medium. It takes into account the variations in resistance to the diffusion due to the tortuosity and to the effects of constriction.

For the gaseous mixture

$$\frac{\partial \bar{\rho}_g}{\partial t} + \frac{\partial}{\partial x}(\bar{\rho}_g^g \bar{v}_g) = \dot{m}. \tag{8}$$

2.3. *Energy conservation equation*

By assuming all the specific heats as constant and with the aid of the mass conservation equations, the energy balance takes a form which is unusual but efficient in the calculations

$$\frac{\partial}{\partial t}(\overline{\rho C_p}\bar{T}) + \frac{\partial}{\partial x}\left(\bar{\rho}_l^l C_{pl}\bar{v}_l\bar{T} + \sum_{j=v,a}\bar{\rho}_j^g C_{pj}\bar{v}_j\bar{T}\right) = \frac{\partial}{\partial x}\left(\lambda_{eff}\frac{\partial \bar{T}}{\partial x}\right) - \Delta h_{vap}^{\circ}\dot{m} \tag{9}$$

here, Δh_{vap}° is a constant defined by

$$\Delta h_{vap}^{\circ} = \Delta h_{vap} + (C_{pl} - C_{pv})\bar{T}$$

λ_{eff} the effective thermal conductivity of the porous medium, Δh_{vap} the enthalpy of vaporization, $\overline{\rho C_p}$ the constant pressure heat capacity of the porous medium

$$\overline{\rho C_p} = \bar{\rho}_s C_{ps} + \bar{\rho}_l C_{pl} + \bar{\rho}_v C_{pv} + \bar{\rho}_a C_{pa}. \tag{10}$$

2.4. *Thermodynamic relations*

The partial pressure of the vapour is equal to its equilibrium pressure

$$\bar{P}_v^g = \bar{P}_{vcq}(T, S). \tag{11}$$

The gaseous mixture is supposed to be an ideal mixture of perfect gases

$$\bar{P}_j = \bar{\rho}_j R\bar{T}/M_j; \quad j = a, v \tag{12}$$

$$\bar{P}_g = \sum_{j=a,v}\bar{P}_j; \quad \bar{\rho}_g = \sum_{j=a,v}\bar{\rho}_j. \tag{13}$$

2.5. *Boundary conditions*

On the adiabatic and impervious face ($x = 0$) the fluxes of heat, air and moisture are null

$$\lambda_{eff}\frac{\partial \bar{T}}{\partial x} + \Delta h_{vap}\bar{\rho}_l^l\bar{v}_l = 0; \quad \bar{v}_a = 0; \quad \bar{\rho}_l^l\bar{v}_l + \bar{\rho}_v^g\bar{v}_v = 0. \tag{14}$$

On the permeable face ($x = L$) the fluxes are continuous and the pressure of the gaseous mixture is constant

$$x = L: \quad \bar{\rho}_l^l\bar{v}_l + \bar{\rho}_v^g\bar{v}_v = \beta|\rho_v^g - \rho_{v\infty}| \tag{15}$$

$$\lambda_{eff}\frac{\partial \bar{T}}{\partial x} + \Delta h_{vap}\bar{\rho}_l^l\bar{v}_l = \alpha|T_\infty - \bar{T}| \tag{16}$$

$$\bar{P}_g^g = P_{atm}. \tag{17}$$

The coefficients of heat exchange α and mass exchange β should be constant.

2.6. *Initial conditions*

Initially, the pressure of the gaseous mixture and temperature are constant in porous media. The distribution of moisture content is that of hydrostatic equilibrium

$$\bar{T} = T_0; \quad \bar{P}_g^g = P_{atm} \tag{18}$$

$$\frac{\partial \bar{P}_c}{\partial x} = \bar{\rho}_l^l g. \tag{19}$$

This equation is associated with a particular condition.

3. NUMERICAL RESOLUTION

The system of the presented equations is solved by a method of finite differences based on the notion of control domain as described by Patankar [11].

This approach has the advantage of assuring the conservation of the fluxes and thus avoiding the generation of parasitical sources.

The domain of integration constitutes a grid of points P_i around which are constructed control domains (Fig. 2). The value of any physical quantity Φ at point P_i and at time $t + \Delta t$ will be noted Φ_i^{n+1}.

The method consists of integrating the conservation equations on the interval $[t, t+\Delta t]$ and on the control domain.

In order to bring the resulting integral equations

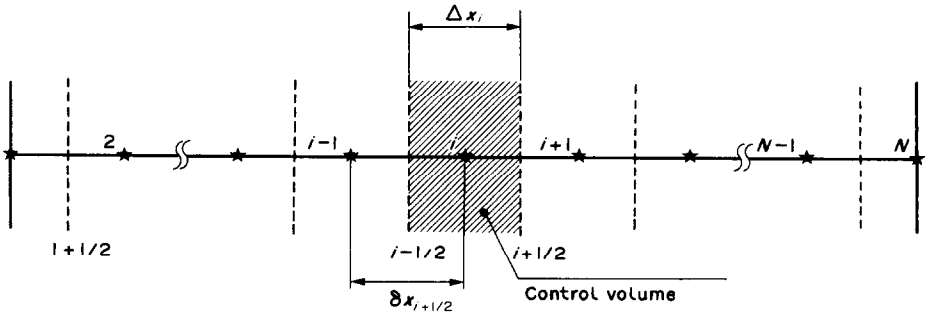

FIG. 2. Numerical grid.

back to algebraic equations tying together the values of the solutions to the nodes on the grid, we make the following hypotheses:

(a) the values of the terms of accumulation $(\partial f/\partial t)_i$ and of the source terms $\dot{m}_i$ and $(\Delta h_{vap}\dot{m})_i$ can be considered as being the averages on the control domain constructed around P_i of $\partial f/\partial t$, $\dot{m}$ and $\Delta h_{vap}\,\dot{m}$.

(b) the source terms, the terms of convection as well as those of diffusion are evaluated at time $t+\Delta t$ (fully implicit scheme).

Taking into account these hypotheses the conservation equations become

$$(\bar{\rho}_{li}^{n+1}-\bar{\rho}_{li}^{n})\frac{\Delta x}{\Delta t}+((\bar{\rho}_l^{l}\bar{v}_l)_{i+1/2}^{n+1}-(\bar{\rho}_l^{l}\bar{v}_l)_{i-1/2}^{n+1})=-\dot{m}_i^{n+1}\Delta x \quad (20)$$

$$(\bar{\rho}_{vi}^{n+1}-\bar{\rho}_{vi}^{n})\frac{\Delta x}{\Delta t}+((\bar{\rho}_v^{g}\bar{v}_v)_{i+1/2}^{n+1}-(\bar{\rho}_v^{g}\bar{v}_v)_{i-1/2}^{n+1})=\dot{m}_i^{n+1}\Delta x \quad (21)$$

$$(\bar{\rho}_{gi}^{n+1}-\bar{\rho}_{gi}^{n})\frac{\Delta x}{\Delta t}+((\bar{\rho}_g^{g}\bar{v}_g)_{i+1/2}^{n+1}-(\bar{\rho}_g^{g}\bar{v}_g)_{i-1/2}^{n+1})=\dot{m}_i^{n+1}\Delta x \quad (22)$$

$$((\rho C_p\bar{T})_i^{n+1}-(\rho C_p\bar{T})_i^{n})\frac{\Delta x}{\Delta t}+\left(\left(\bar{\rho}_l^{l}C_{pl}\bar{v}_l\bar{T}+\sum_{j=v,a}\bar{\rho}_j^{g}C_{pj}\bar{v}_j\bar{T}\right)_{i+1/2}^{n+1}-\left(\bar{\rho}_l^{l}C_{pl}\bar{v}_l\bar{T}+\sum_{j=v,a}\bar{\rho}_j^{g}C_{pj}\bar{v}_j\bar{T}\right)_{i-1/2}^{n+1}\right)=\left(\lambda_{eff}\frac{\partial\bar{T}}{\partial x}\right)_{i+1/2}^{n+1}-\left(\lambda_{eff}\frac{\partial\bar{T}}{\partial x}\right)_{i-1/2}^{n+1}-\Delta h_{vap}\dot{m}_i^{n+1}\Delta x. \quad (23)$$

On the surfaces of the porous medium, the equations are rendered discrete by integrating over half the control domain and by taking the boundary conditions into account.

The different parameters are calculated over the faces of the control domains, their variations being taken as linear.

The primary derivations are approximated over two nodes within the porous medium

$$\left(\frac{\partial f}{\partial x}\right)_{i+1/2}^{n+1}=(f_{i+1}^{n+1}-f_i^{n+1})/\delta x. \quad (24)$$

For greater precision, they are approximated over three nodes on the permeable surface

$$\left(\frac{\partial f}{\partial x}\right)_N^{n+1}=(-3f_N^{n+1}+4f_{N-1}^{n+1}-f_{N-2}^{n+1})/2\delta x. \quad (25)$$

Convection in the energy equation is calculated by an upwind scheme [11].

Given the strongly non-linear nature of the equations, an iterative Newton's method is used in association with under-relaxation.

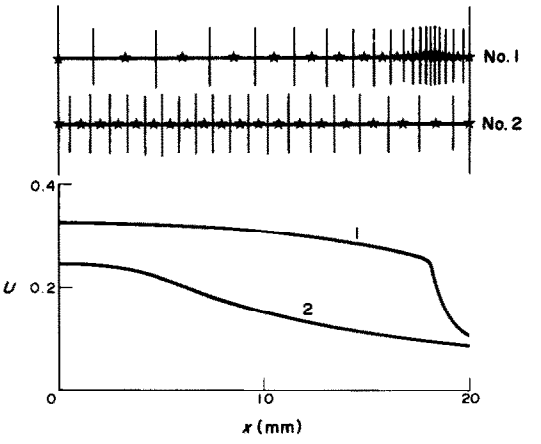

FIG. 3. Adaptation of grid to moisture profile.

The simulation of the drying process sometimes gives rise to steep drying fronts. With a view to attaining greater precision without increasing the number of nodes in the grid, an algorithm distributes the nodes in relation to the humidity profile (Fig. 3). The grid is recalculated during the drying process whenever the slope or the position of the front changes significantly.

4. RESULTS

4.1. *Description of drying process*

The numerical model is applied to the drying of two different porous media (clay brick and softwood). The physical characteristics of these media are detailed in the Appendix. The results obtained make it possible to analyse precisely the different mechanisms involved in each drying phase.

4.1.1. *Period of constant drying rate.* At the start of drying, when the initial water content is sufficient, the porous medium approaches the temperature of the wet bulb. During this transition phase, the higher the initial temperature is, the greater the drying rate (Fig. 4).

When the drying becomes stable, the temperature is uniform within the porous medium. The flow of vapour being negligible in the core of the medium, evaporation only takes place at the surface. The boundary conditions become

$$(T_\infty-\bar{T})=\beta\Delta h_{vap}(\bar{\rho}_{vs}^{g}(\bar{T})-\rho_{v\infty}). \quad (26)$$

The drying rate is proportional to the heat supplied

$$D_r=\frac{\alpha}{\Delta h_{vap}}(T_\infty-\bar{T}). \quad (27)$$

Given the characteristics of the air flow, we can see on equation (27) that the drying rate D_r depends on α and T. In the plane (ρ_v, T), point E with coordinates $(\rho_{v\infty}, T_\infty)$ characterizes the external air flow. Point P with coordinates $(\bar{\rho}_{vs}^{g}, \bar{T})$, which characterizes the surface of the porous medium, is obtained by crossing

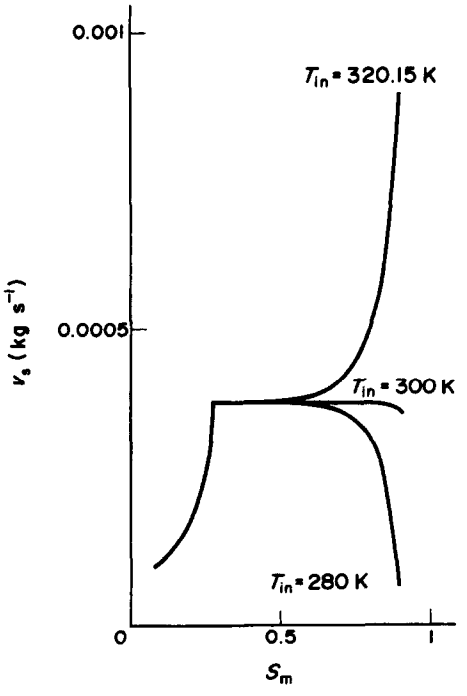

FIG. 4. Drying rate for brick ($T_\infty = 360.15$ K, $H_r = 0$, $\alpha = 15$ W m^{-2} K^{-1}, $\beta = 0.014$ m s^{-1}).

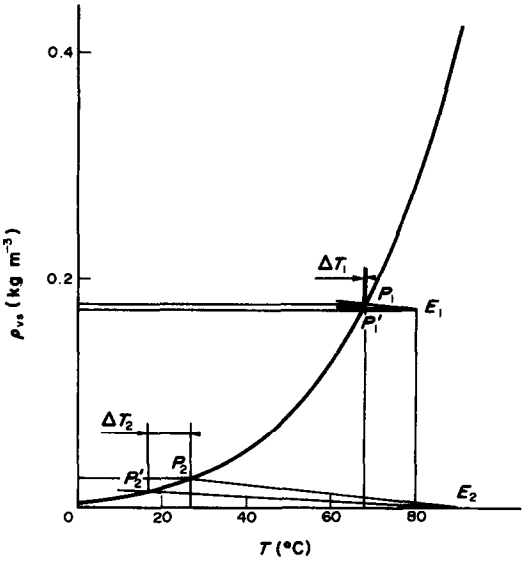

FIG. 5. Graphical determination of interface conditions.

the saturation curve with the line of slope $-(\alpha/\beta)\Delta h_{vap}$ coming from E (Fig. 5).

Thus, given $\rho_{v\infty}$ and T_∞, the determination of the equilibrium temperature $\bar{T}$ needs the knowledge of the ratio β/α.

Equation (27) allows an accurate experimental determination of the heat exchange coefficient α. On the other hand, given the very low difference between $\bar{\rho}^g_{vs}$ and $\rho_{v\infty}$, the mass exchange coefficient β is really difficult to measure. The ratio β/α is often given by the analogy between the transfers.

Nevertheless, this analogy is valid only when the vapour pressure is negligible with regard to the total pressure: between 65 and 95°C, the ratio β/α increases by a factor of about 5 [12].

It is also of great interest to study separately the influence of coefficients α and β.

When the equilibrium temperature $\bar{T}$ is sufficiently high, it is only slightly affected by the term $-(\alpha/\beta)\Delta h_{vap}$ (point 1 in Fig. 5). The simulations confirm that, in such conditions, the drying rate depends only slightly on β and is mainly proportional to α (Fig. 6).

For small values of $\bar{T}$, the slope of the saturation curve is weak. The equilibrium temperature becomes sensitive to the term $-(\alpha/\beta)\Delta h_{vap}$ (point 2 in Fig. 5) and each of the exchange coefficients has an influence on the drying rate. However, in these cases, the vapour pressure is much lower than the total pressure: the ratio β/α can be precisely calculated by the analogy between the transfers.

Finally, for all temperatures below the boiling point, β can be determined by the analogy between the transfers without significant error.

During this period of constant drying rate, the increase in the volume of gas carried by liquid extraction tends to subject the medium to partial vacuum (Figs. 7 and 8). This lowering of pressure restrains the moisture movement. The one persists while the moisture flows essentially by capillary action.

4.1.2. *Period of decreasing drying rate.* When the liquid phase becomes discontinuous, the liquid migration stops (pendular state). Thus, the moisture content decreases notably at the surface of the medium which becomes hygroscopic. The pressure of the vapour at the interface, and thus the drying rate, decreases. The gradient of vapour pressure generates gaseous diffusion towards the surface and evaporation inside the porous medium. During this period, the evaporation propagates a zone in which the gradient of moisture content is very high (drying front) towards the impervious surface of the slab.

The temperature rises throughout the porous medium. The discontinuity of the temperature gradient close to the front (Figs. 7(a) and 8(a)) is a result of the heat flux necessary for evaporation and of the change in effective thermal conductivity. A pressure gradient is observed between the front and the surface (Figs. 7(c) and 8(c)). This results from the resistance of the porous medium to the gas migration generated by diffusion. In the model, this effect is formulated by Darcy's law (3). Between the drying front and the impervious surface, a slight convection of the gaseous phase and the rise in temperature cause the pressure to level out at its value on the front. The value of this pressure becomes even more important as the drying rate increases and as the permeability of the gaseous phase weakens.

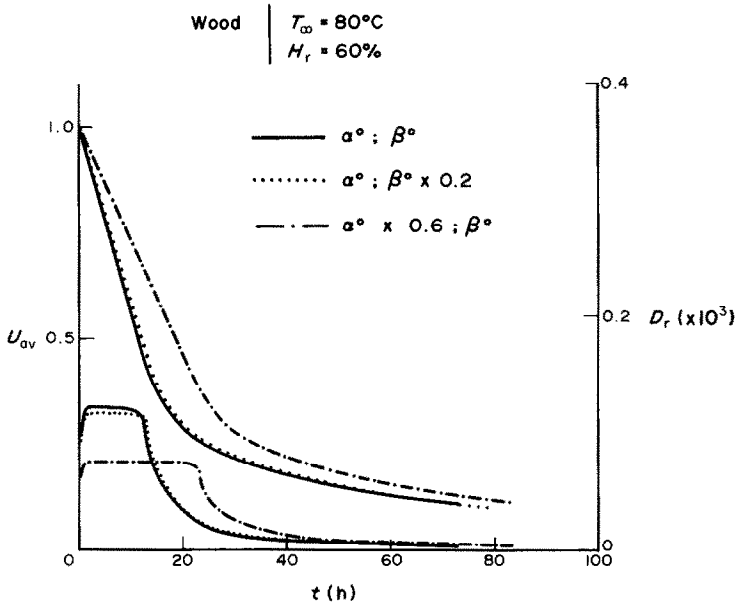

FIG. 6. Influence of exchange coefficients ($T_\infty = 80°C$, $H_r = 60\%$, $T_{ini} = 65°C$, $\alpha° = 23$ W m^{-2} K^{-1}, $\beta° = 0.02$ m s^{-1}).

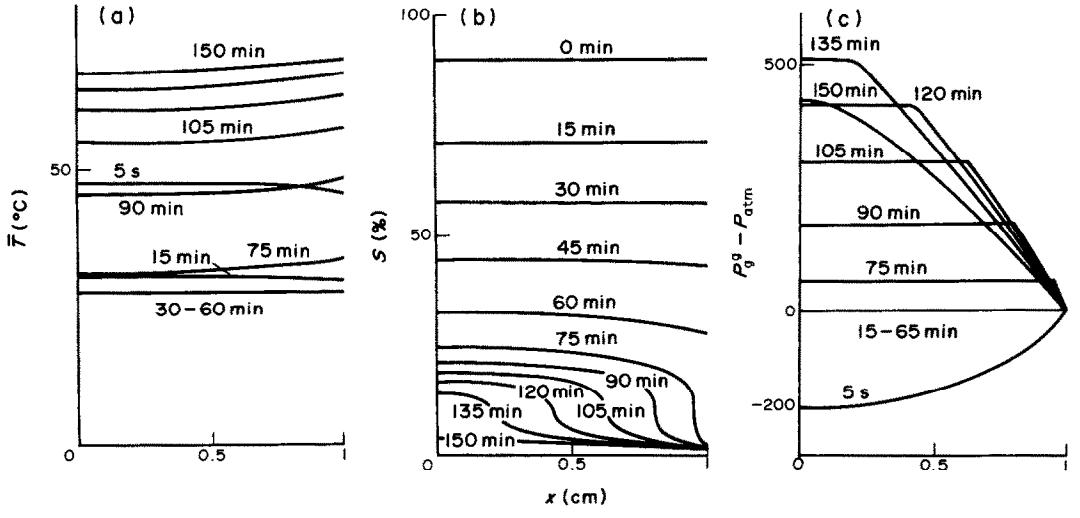

FIG. 7. Temperature (a), saturation (b), and pressure (c) profiles for brick ($T_\infty = 360.15$ K, $H_r = 0$, $T_{ini} = 320.15$ K, $\alpha = 15$ W m^{-2} K^{-1}, $\beta = 0.014$ m s^{-1}).

As the front separates from the interface, the steepness in the moisture content profile becomes smaller, temperature and pressure higher. When the front reaches the impervious surface, the entire porous medium is in the hygroscopic zone (third drying period). The pressure of the gaseous phase decreases. Temperature, moisture content and pressure approach respectively, ambient temperature, equilibrium moisture content and atmospheric pressure.

4.2. *Sensitivity to transport parameters*

The aim of this study is to gain an idea of the allowable errors at the time of the evaluation of the transport parameters.

4.2.1. *Effective diffusivity of vapour.* In the domain of liquid migration, the vapour pressure is equal to the saturate vapour pressure of which the gradient is negligible. Therefore, the effective diffusivity has no influence upon drying. On the other hand in the hygroscopic domain, the value of this coefficient directly controls the migration of moisture. However, the character of the transport does not become changed: it is interesting to note that two proportional values of D_{eff} give, for the same average saturation (therefore at different moments) the same water content profiles (Fig. 9).

4.2.2. *Effective thermal conductivity.* Results obtained with a conductivity λ_{eff} twice as great show

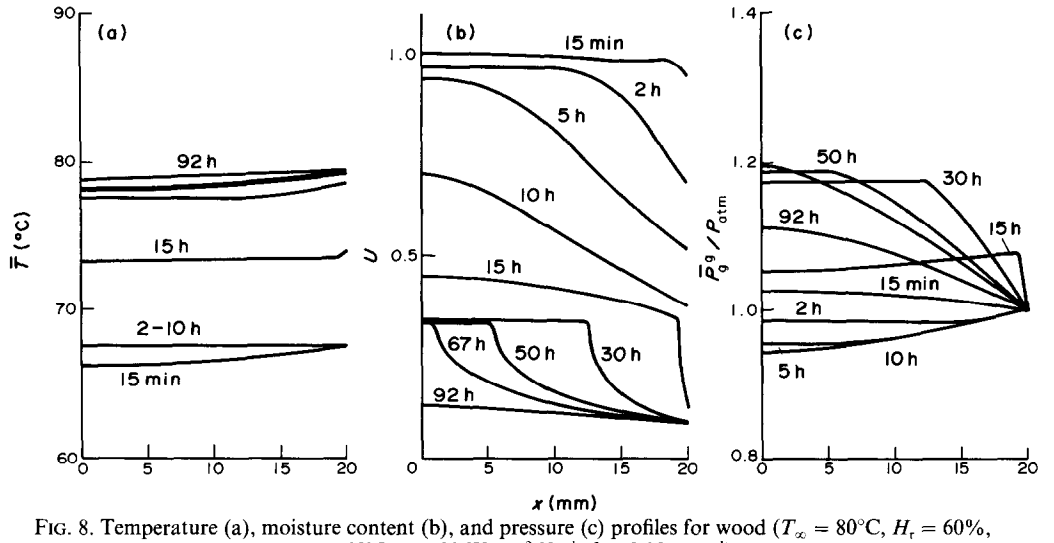

FIG. 8. Temperature (a), moisture content (b), and pressure (c) profiles for wood ($T_\infty = 80°C$, $H_r = 60\%$, $T_{ini} = 65°C$, $\alpha = 23\ W\ m^{-2}\ K^{-1}$, $\beta = 0.02\ m\ s^{-1}$).

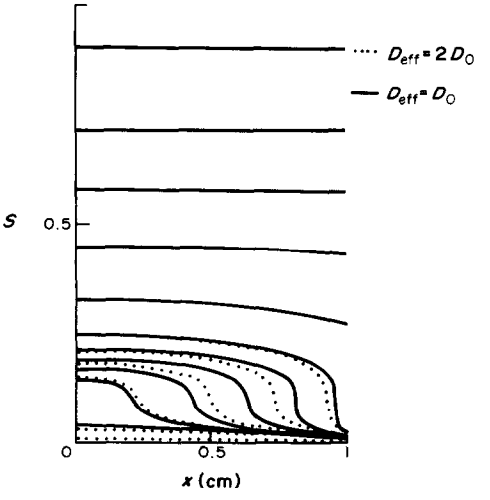

FIG. 9. Influence of effective diffusivity (brick).

that the model is not very sensitive to this parameter. As thermal conductivity is significant in regard to existing thermal fluxes, the resistance of the porous medium to heat transfer, and thus the temperature gradient are always low. Despite considerable variations in λ_{eff}, the influence of this gradient on moisture transfer remains negligible in the liquid phase as well as in the gaseous phase.

4.2.3. *Intrinsic permeability*. The intrinsic permeability characterizes the aptitude of a single fluid phase to migrate within the porous medium. In the case of drying where two fluid phases exist together, this parameter is used for the calculation of the relative permeability to each phase.

Generally the greater the intrinsic permeability is, the lower the gradients of pressure and of moisture content are (Fig. 10). In the domain of liquid migration, the influence of this parameter is perceptible only when the moisture profile is far from the hydrostatic profile. The duration of the constant drying rate period increases when K increases since the interface later becomes hygroscopic. In the hygroscopic domain, K determines the interaction between gaseous diffusion and the gradient of gaseous phase pressure (see Section 5.2).

4.2.4. *Relative permeabilities*. These parameter functions of relative saturation determine the resistance to migration of each phase (liquid and gas) with regard to those where the porous medium is fully saturated. They have a significant influence especially in the zones where these values are very low (near the fully saturated state for K_g and the end of the funicular state for K_l). It is to be noted that the experimental detection of very low permeability is extremely difficult: it is generally taken as equal to zero in a drying model. Calculations show however that, when one attributes values that are very low but nonzero to permeabilities, then the moisture content profiles change considerably.

Thus, in the case of wood, the few pits which are located on the lateral cell walls cannot be ignored. The geometrical model inspired by Comstock and taken up by Spolek and Plumb [13] is used here without making the assumption that all the pits are on the overlapped surfaces (Fig. 11(a)). The permeability to the gaseous phase is no longer strictly null above irreducible saturation and the phenomenon of the trapping of the gaseous phase disappears (Fig. 11(b)).

The considerable differences obtained in moisture profiles show the influence of the gaseous phase on liquid migration and thus, the necessity for certain porous media that the drying model take into account the gaseous pressure.

Concerning liquid permeability the value of irreducible saturation (saturation below which liquid permeability is equal to zero) takes a prominent part in the transition between liquid migration and transport by gaseous diffusion. Thus the further the pendular state begins from the hygroscopic range, the greater the evaporation front steepens (Fig. 12).

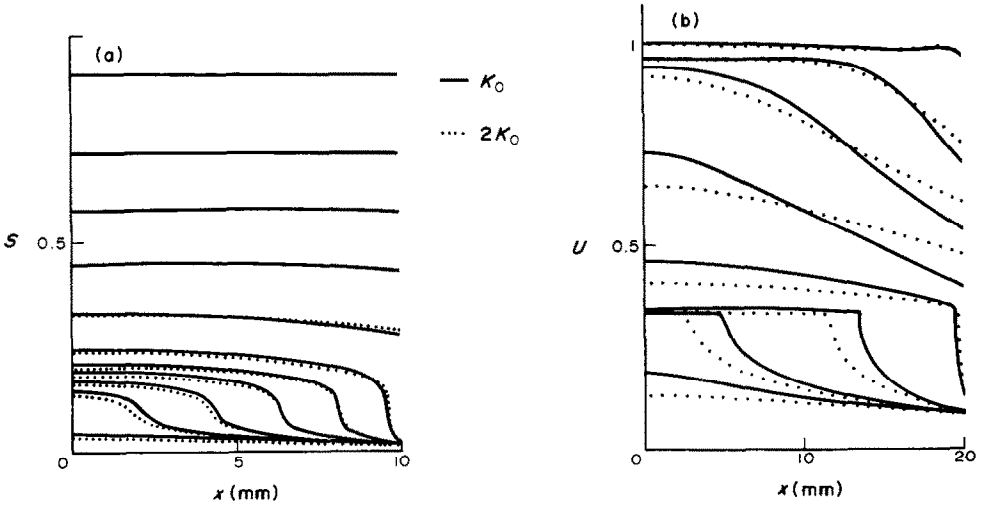

FIG. 10. Influence of intrinsic permeability: comparison between (a) brick and (b) wood.

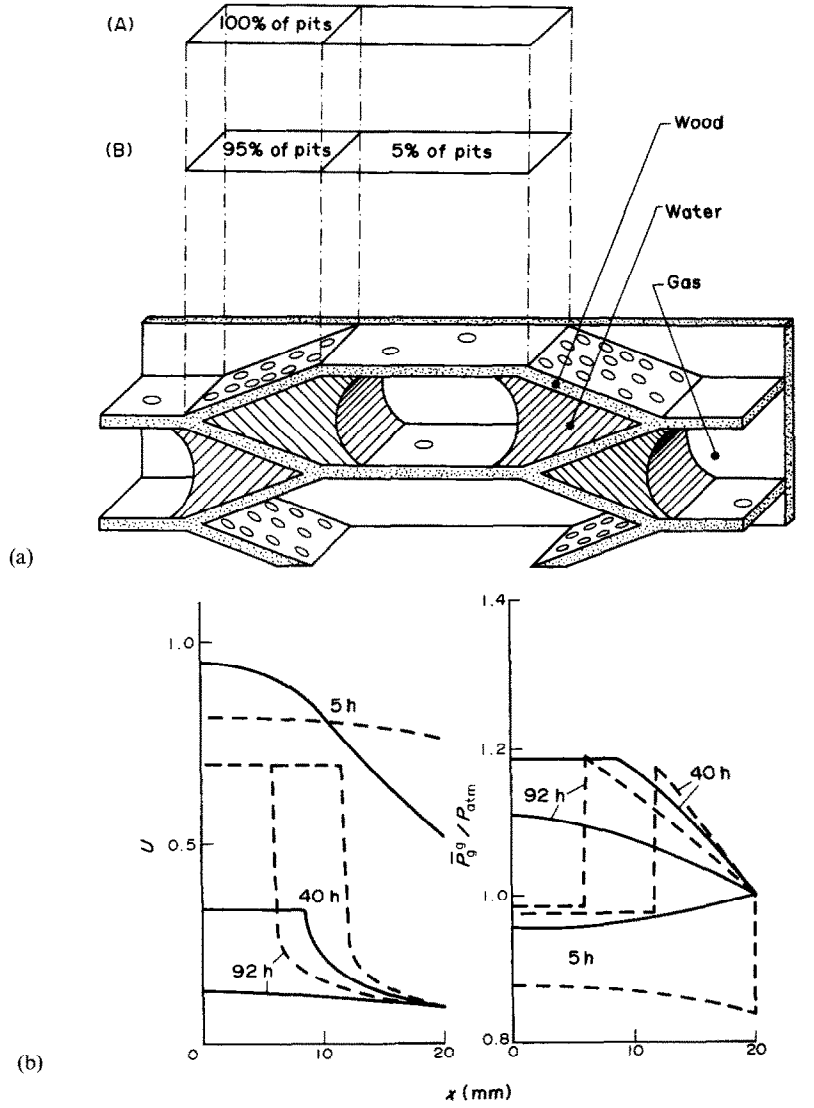

FIG. 11. Effect of relative permeability to gaseous phase (wood): (a) geometrical model; (b) numerical simulations. ----, All the pits are assumed to be on the overlapped surfaces (case A). ——, Of the pits 5% are on the lateral walls of the tracheids (case B).

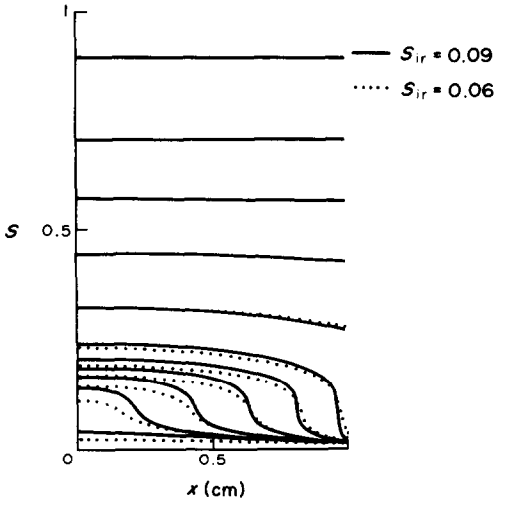

FIG. 12. Influence of irreducible saturation (brick).

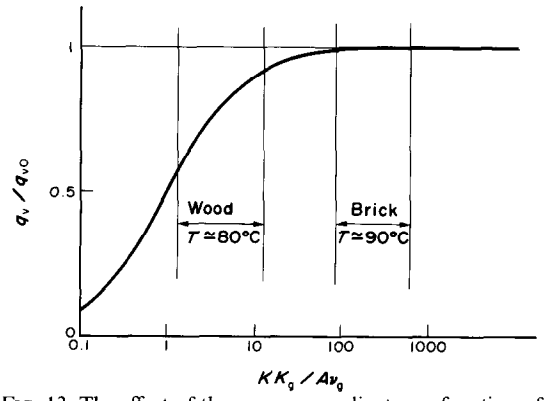

FIG. 13. The effect of the pressure gradient as a function of physical characteristics and drying conditions.

5. REDUCTION OF THE MODEL

5.1. *Heat transport by convection*

The energy conservation equation (9) can take the usual form

$$\rho C_p \frac{\partial \bar{T}}{\partial t} + \left(\bar{\rho}_l^l C_{pl} \bar{v}_l + \sum_{j=a,v} \bar{\rho}_j^g C_{pj} \bar{v}_j\right) \frac{\partial \bar{T}}{\partial x} = \frac{\partial}{\partial x}\left(\lambda_{eff} \frac{\partial \bar{T}}{\partial x}\right) - \Delta h_{vap} \dot{m}. \quad (28)$$

Drying was simulated with and without the terms of heat transport by convection obtained in this equation. The change in temperature gradient, even when the latter is at its highest (transient period) remains less than 1% and the change in total drying time is a mere 0.5%.

Also for forced convection drying below the boiling point these terms in energy balance can be left out. It is interesting to specify that the terms of equation (9)

$$\frac{\partial}{\partial x}\left(\bar{\rho}_l^l C_{pl} \bar{v}_l \bar{T} + \sum_{j=a,v} \bar{\rho}_j^g C_{pj} \bar{v}_j \bar{T}\right)$$

are more important and neglecting them can lead to appreciable errors.

5.2. *Conservation equation of gaseous phase*

The dry air flux ($\bar{\rho}_a^g \bar{v}_a$) is often weak compared to vapour flux. Taking $\bar{\rho}_a^g \bar{v}_a = 0$ leads to a new expression of the vapour flux

$$\bar{\rho}_v^g \bar{v}_v = -\frac{\bar{\rho}_g^g}{(1-\bar{\rho}_v/\bar{\rho}_g)} D_{eff} \frac{\partial}{\partial x} \frac{\bar{\rho}_v}{\bar{\rho}_g} = q_v. \quad (29)$$

Developing the gradient with the aid of the relationships of perfect gases (12) and (13) and using Darcy's law (3) to express the term $(\partial/\partial x)\bar{P}_g^g$ make it possible to write the vapour flux as follows:

$$q_v = \frac{q_{v0}}{(1 + Av_g/KK_g)} \quad (30)$$

with

$$A = \frac{\bar{\rho}_g^g}{(1-\bar{\rho}_v/\bar{\rho}_g)} D_{eff} \frac{M_a M_v \bar{p}_v^g}{(\bar{p}_a^g M_a + \bar{p}_v^g M_v)^2} \quad (31)$$

and

$$q_{v0} = -A \frac{\bar{p}_g^g}{\bar{p}_v^g} \frac{\partial}{\partial x} \bar{p}_v^g \quad (32)$$

where q_{v0} is the vapour flux obtained by taking the gaseous pressure as constant. The value of q_v is always less than q_{v0}. The difference between these two fluxes results from the inhibition of the diffusion by the total pressure gradient (term $\bar{\rho}_g$ in the gradient of equation (29)). It is worth noting that this gradient of the total pressure results, through Darcy's law, from the resistance of the porous medium to the barycentric motion of the gaseous phase generated by diffusion.

Figure 13 shows those values of Av_g/KK_g for which the pressure gradient influence is negligible. In such cases, the pressure of the gaseous phase is taken equal to atmospheric pressure. Darcy's law and mass conservation for the gaseous phase can be discarded. The simulation shows that these two assumptions give very close results for brick (error less than 1%).

In the case of wood, the resistance of the porous medium to gaseous migration is very important. The pressure gradient generated by the diffusive flux of vapour is too great to be neglected (Figs. 13 and 14). However, when gaseous pressure has no effect on liquid migration (pendular state) a good approximation is obtained by correcting the diffusivity with multiplying factor

$$\left(1 + \frac{Av_g}{KK_g}\right)^{-1}.$$

6. CONCLUSION

The aim of this study is to describe heat and mass transfer during drying by forced convection of porous media. The model used is very comprehensive. Sim-

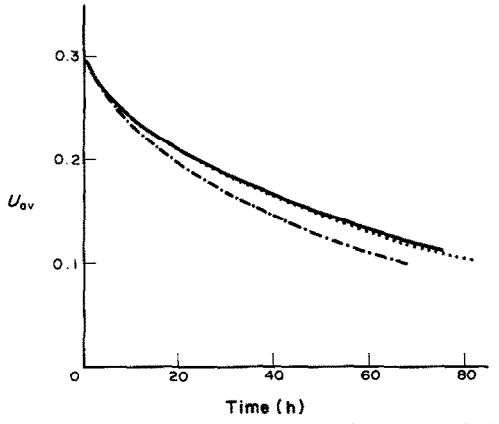

FIG. 14. The effect of the pressure gradient upon drying (wood): ——, complete model; —·—, $\bar{\rho}_a\bar{v}_a = 0$, $\bar{p}_g^g = \rho_{atm}$; – – –, $\bar{\rho}_a\bar{v}_a = 0$, $\bar{P}_g^g = P_{atm}$, $D_{eff} = D_{eff}/(1 + Av_g/KK_g)$.

plistic assumptions have been avoided, especially insofar as the effect of gaseous pressure is concerned. This model is numerically resolved and the drying process is simulated for two very different porous media. The temperature remains below the boiling point.

This study permitted the selection of the parameters for which the model is most sensitive. Among different physical characteristics of porous media, the model is sensitive to permeabilities and to effective diffusivity, i.e. to those parameters which characterize moisture migration fitness.

On the other hand, at the interface, the drying is principally controlled by the heat exchange coefficient. The resistance to mass transfer proved negligible, especially as the equilibrium temperature increases.

Greater insight into important phenomena such as gaseous pressure has been obtained by comparing the results for two different porous media. When gaseous permeability is weak, taking the total pressure of the gaseous phase into account reduces liquid migration as well as vapour diffusion.

Finally, we have determined the conditions for which certain reductions of the model lead to good approximations. The simplifications made are significant as they obviate the need to calculate pressure and heat transport by convection.

Acknowledgement—This work was supported by the Technical Centre of Wood and Furniture (Centre Technique du Bois et de l'Ameublement, Paris, France). The authors wish also to thank their colleagues from the Centre for helpful discussions.

REFERENCES

1. S. Whitaker, Simultaneous heat and momentum transfer in porous media: a theory of drying. In *Advances in Heat Transfer*, Vol. 13, pp. 119–203. Academic Press, New York (1977).
2. S. Whitaker and W. Chou, Drying granular porous media—theory and experiment, *Drying Technol.* **1**, 3–33 (1983).
3. S. Whitaker and S. Chen, Moisture distribution during the constant rate drying period for unconsolidated porous media: failure of the diffusion theory, *Proc. 5th Int. Drying Symp.*, Cambridge, Massachusetts, pp. 39–48 (1986).
4. S. Bories, G. Bacon and M. Recan, Experimental and numerical study of coupled heat and mass transfer in porous materials, *Proc. 4th Int. Drying Symp.*, Kyoto, pp. 159–164 (1984).
5. C. Moyne and A. Degiovanni, Importance of gas phase momentum equation in drying above the boiling point of water, *Proc. 4th Int. Drying Symp.*, Kyoto (1984).
6. C. Basilico and M. Martin, Approche expérimentale des mécanismes de transfert au cours du séchage convectif à haute température d'un bois résineux, *Int. J. Heat Mass Transfer* **27**, 657–668 (1984).
7. O. A. Plumb, G. A. Spolek and B. A. Olmstead, Heat and mass transfer in wood during drying, *Int. J. Heat Mass Transfer* **28**, 1669–1678 (1985).
8. T. Z. Harmathy, Simultaneous moisture and heat transfer in porous system with particular reference to drying, *Int. Engng Chem. Fund.* **8**(1), 92–103 (1969).
9. C. L. D. Huang, Multi-phase moisture in porous media subjected to temperature gradient, *Int. J. Heat Mass Transfer* **22**, 1295–1307 (1979).
10. C. L. D. Huang, H. H. Siang and C. H. Best, Heat and moisture transfer in concrete slabs, *Int. J. Heat Mass Transfer* **22**, 257–266 (1979).
11. S. V. Patankar, *Numerical Heat Transfer and Fluid Flow*. Hemisphere/McGraw-Hill, New York (1980).
12. J. F. Sacadura, *Initiation aux transfers thermiques*. Technique et Documentation, Paris (1982).
13. G. A. Spolek and O. A. Plumb, Capillary pressure in softwood, *Wood Sci. Technol.* **15**, 189–199 (1981).
14. A. E. Scheidegger, *The Physics of Flow through Porous Media*, 3rd Edn. University of Toronto Press, Toronto (1974).
15. L. D. Baver and W. H. Garner, *Soil Physics*, 4th Edn. Wiley, New York (1972).
16. W. D. Kingeny, H. R. Bower and D. R. Uhlman, *Introduction to Ceramics*, 2nd Edn. Wiley Intersciences, New York (1976).
17. J. F. Siau, *Flow in Wood*. Syracuse University Press, New York (1971).
18. G. L. Comstock, Moisture diffusion coefficients in wood as calculated from absorption, desorption and steady state data, *Forest Prod. J.* 97–103 (1963).
19. C. Moyne, Contribution à l'étude du transfert simultané de chaleur et de masse lors du séchage sous vide d'un bois résineux, Thèse de Docteur-Ingénieur, Nancy (1982).

APPENDIX (PHYSICAL CHARACTERISTICS)

(Units are specified in nomenclature. $\bar{T}$ in Kelvin)

1. *Brick*

$$\varepsilon = 0.26; \quad K = 2.5 \times 10^{-14}; \quad \rho_s = 2600;$$
$$C_{ps} = 879; \quad \lambda_s = 1.442.$$

Capillary pressure (deduced from empirical Levret approach) [14]

$$p_c = \varepsilon\sigma J(S)/K$$

where

$$J(S) = 0.364(1 - \exp(-40(1-S))) + 0.221(1-S) + 0.005/(S - 0.08).$$

Relative permeabilities [14]

$$K_g = 1 - 1.1S, \qquad S < S'_{ir} = 1/1.1$$
$$K_g = 0, \qquad S > S'_{ir}$$

$$K_l = (S - S_{ir})/(1 - S_{ir}), \quad S > S_{ir} = 0.09$$
$$K_l = 0, \quad S < S_{ir}.$$

Effective diffusivity [15]

$$D_{eff} = D(1-S)^2 \varepsilon_g^{4/3}.$$

Effective thermal conductivity [16]

$$\lambda_{eff} = (\lambda_g^n \varepsilon_g + \lambda_l^n \varepsilon_l + \lambda_s^n (1-\varepsilon))^{1/n} \quad \text{with} \quad n = 0.25.$$

Vapour pressure [8]

$$\bar{p}_v = \bar{p}_{vs} \exp(-2\sigma M_v / r \rho_l R \bar{T})$$

with

$$\log(r) = 2.16\,10^{-2} + 43.8S - 253.5S^2 + 794.54S^3 - 1333.7S^4 + 1111S^5 - 352.5S^6 - 10.$$

2. *Softwood*

$$\varepsilon = 0.66; \quad K = 10^{-16}; \quad \rho_s = 500, \quad C_{ps} = 1400.$$

Capillary pressure [13]

$$p_c = \sigma\, 1.364 \times 10^5 U_l^{-0.63}, \quad U_l = U - U_{psf}.$$

Effective diffusivity [17, 18]

$$D_{eff} = K_g (D/45).$$

Relative permeabilities [7]

	K_g	K_l
$U < U_{psf}$	1	0
$0 < U_l < U_{ir}$	$0.95(1-\sqrt{(U_l/U_{ir})})+0.05$	0
$U_{ir} < U_l < U_{cr}$	0.05	$0.95(\sqrt{(U_l/U_{ir})}-1)$
$U_{cr} < U_l$	$0.05\left(1-\frac{U_l-U_{cr}}{U_{sat}-U_{cr}}\right)$	$0.95+0.05\frac{U_l-U_{cr}}{U_{sat}-U_{cr}}$

Effective thermal conductivity [19]

$$U > 0.4: \quad \lambda_{eff} = (0.0065/U + 0.0932)(0.986 + 2.7U) \times (3.55 + 3.65\bar{T})10^{-3}$$
$$U < 0.4: \quad \lambda_{eff} = (0.129 - 0.049U)(0.986 + 2.7U) \times (1 + (2.05 + 4U)(\bar{T} - 273) \times 10^{-3}).$$

Vapour pressure [19]

$$p_v = p_{vs} \exp((17.884 - 0.1423\bar{T} + 0.0002363\bar{T}^2)(1.0327 - 0.000674\bar{T})^{92U}).$$

Fibre saturation point [17]

$$U_{psf} = 0.598 - 0.001\bar{T}.$$

LE SÉCHAGE CONVECTIF DE MILIEUX POREUX : ÉTUDE DÉTAILLÉE D'UN MODÈLE DE TRANSFERT DE CHALEUR ET DE MASSE

Résumé—La formulation des transferts couplés de chaleur et de masse utilisée ici est issue de la théorie de Whitaker. Le système d'équations, très général, prend notamment en compte l'effet de la pression de la phase gazeuse. Il est utilisé pour simuler numériquement le séchage de deux milieux poreux fort différents, dans le cas de transferts monodimensionnels. La température reste inférieure au point d'ébullition. Les résultats montrent l'évolution des profils internes de chacune des variables (température, teneur en eau et pression) ainsi que les cinétiques de séchage. La comparaison entre les deux milieux permet de mieux appréhender la sensibilité de modèle aux paramètres internes et aux conditions à l'interface ainsi que l'à-propos de certaines réductions du modèle.

DETAILLIERTE UNTERSUCHUNG EINES MODELLS FÜR DEN WÄRME- UND STOFFTRANSPORT BEI DER KONVEKTIVEN TROCKNUNG PORÖSER MEDIEN

Zusammenfassung—Das hier verwendete Modell für den Wärme- und Stofftransport in porösen Medien ist von der Whitaker-Theorie abgeleitet. Sie führt zu einem sehr umfassenden Gleichungssystem und berücksichtigt den Effekt des Gasdrucks. Die numerische Lösung erfolgt mit eindimensionaler Übertragung. Für zwei sehr unterschiedliche poröse Medien werden der Verlauf von Temperatur, Wassergehalt und Druck sowie die Kinetik des gesamten Trocknungsvorgangs berechnet. Mit diesem Hilfsmittel können die Auswirkung von internen Parametern und Bedingungen an der Grenzfläche auf das Modell sowie die Auswirkung bestimmter Vereinfachungen im Modell untersucht werden.

ИССЛЕДОВАНИЕ МОДЕЛИ ТЕПЛО- И МАССОПЕРЕНОСА ПРИ КОНВЕКТИВНОЙ СУШКЕ ПОРИСТОЙ СРЕДЫ

Аннотация—Используемая в данной работе модель тепло- и массопереноса выводится из теории Витаккера. В результате получается замкнутая система уравнений, в которой учитывается эффект давления газа. Одномерная система решается численно. Для двух существенно отличающихся по своим свойствам пористых сред рассчитывается эволюция во времени полей температуры, влагосодержания, давления пара, а также интегральные кинетические характеристики процесса сушки. Данный метод расчета позволяет исследовать чувствительность модели к влиянию внутренних параметров и условий на границе раздела, так же как и эффект некоторых упрощений в модели.